Transfer reactions with heavy ions on light nuclei*

K. G. Nair, H. Voit,† C. W. Towsley, M. Hamm, J. D. Bronson, and K. Nagatani
Cyclotron Institute, Texas A&M University, College Station, Texas 77843
(Received 7 July 1975)

Proton and neutron transfer reactions resulting from the bombardment of ^{12}C and ^{16}O targets by ^{14}N beams and ^{12}C, ^{14}N, and ^{16}O targets by ^{10}B beams have been studied with counter telescopes and particle identification techniques. The incident energies were far above the Coulomb barrier for these systems: 155 MeV for ^{14}N ions and 100 MeV for ^{10}B ions. Angular distributions have been measured for transitions to the ground states and several excited states in the residual nuclei produced. Ejectile excitations were also observed in some instances. Exact finite range distorted-wave–Born-approximation calculations have been performed for these states which are mostly in the $1p$ and $2s$-$1d$ shells. The extracted spectroscopic factors are generally in good agreement with theoretical predictions and other previously obtained results. However, there are some conspicuous but isolated instances where they are not, pointing towards a need for more sophisticated approaches including core excitations for those cases. Generally the quality of spectroscopic studies with heavy-ion-induced transfer reactions is comparable if not superior to that from the corresponding light-ion-induced reactions.

[NUCLEAR REACTIONS $^{12}C(^{14}N,^{13}N)$, $^{12}C(^{14}N,^{13}C)$, $E=155$ MeV; $^{16}O(^{14}N,^{13}N)$, $^{16}O(^{14}N,^{13}C)$, $^{16}O(^{14}N,^{15}N)$, $E=155$ MeV; $^{12}C(^{10}B,^{11}B)$, $^{12}C(^{10}B,^{11}C)$, $E=100$ MeV; $^{14}N(^{10}B,^{11}B)$, $^{14}N(^{10}B,^{11}C)$, $^{14}N(^{10}B,^{9}Be)$, $E=100$ MeV; $^{16}O(^{10}B,^{11}B)$, $^{16}O(^{10}B,^{11}C)$, $^{16}O(^{10}B,^{9}Be)$, $E=100$ MeV; measured $\sigma(\theta)$; EFR DWBA analyses; extracted spectroscopic factors.]

I. INTRODUCTION

The present study was undertaken to test the validity of the exact finite range (EFR) distorted-wave–Born-approximation (DWBA) theory in analyzing data on one-nucleon transfer reactions in light nuclei at energies far above the Coulomb barrier. Therefore, the emphasis here is not on discovering new levels or making new spin-parity assignments but rather on applying the theory to a number of fairly well-known transitions in light nuclei. The credibility of these results is enhanced because of the possibility of cross checking from the number of different reactions studied.

Studies similar to the present one have been conducted by Tamura and Low,[1] Ford *et al.*,[2] and Becchetti *et al.*[3] in medium-heavy and heavy elements. Anyas-Weiss *et al.*[4] have conducted extensive investigations on heavy-ion reactions in light nuclei, but their analyses have been mostly based on semiclassical recipes. However, the latter authors emphasize the selectivity of heavy-ion reactions and have presented a variety of very useful systematics. Previous experimental studies of the $^{12}C(^{14}N,^{13}N)^{13}C$ and $^{12}C(^{14}N,^{13}C)^{13}N$ reactions have been performed by von Oertzen *et al.*[5] at 78 MeV. DeVries *et al.*[6] have investigated the $^{12}C(^{14}N,^{13}N)^{13}C$ reaction at an incident energy of 100 MeV.

In Secs. II and III we summarize the experimental procedures and results, respectively. Section IV deals with the details of the EFR DWBA analysis, and Sec. V concerns the application of theory to the experimental angular distributions. We present a discussion of the extracted spectroscopic factors in Sec. VI and the concluding remarks in Sec. VII.

II. EXPERIMENTAL PROCEDURES

The incident $^{14}N^{4+}$ and $^{10}B^{3+}$ ions were accelerated by the Texas A&M variable energy cyclotron. The analyzed beam had an estimated energy uncertainty of ±0.5%, but this uncertainty should not affect the present results due to the expected slow variation of cross sections with incident energy. Typical currents were approximately 200 nA on target. The ^{12}C targets used for these experiments were 430 $\mu g/cm^2$ natural carbon foils. For the ^{14}N and ^{16}O targets, a gas cell operating at a pressure of 180 Torr was used. The beam entrance and exit windows were 1.1 mg/cm^2 nickel and 2.1 mg/cm^2 Havar foils, respectively. Reaction products were detected after they passed through a 450 $\mu g/cm^2$ Mylar window in the cell. The detected particles were identified in a counter telescope consisting of three solid-state surface barrier detectors of typical thicknesses 50, 50, and 2000 μm for $\Delta E1$, $\Delta E2$, and E signals, respectively.

Particle identification (PID) functions of the form

$$\mathrm{PID} = \Delta E(E + k\Delta E + E_0)$$

were electronically generated by hardware from the E and ΔE pulses. The constants k and E_0 were suitably adjusted so that the PID function depends essentially only on the particle type and not its energy. A typical particle identification spectrum thus obtained in the $^{14}N + ^{16}O$ experiment is shown in Fig. 1. Two such functions were generated from the combinations

$$\mathrm{PID1} = \Delta E1[(E + \Delta E2) + k\Delta E1 + E_0],$$

$$\mathrm{PID2} = \Delta E2[E + k\Delta E2 + E_0].$$

The pulses corresponding to PID2 were then used to gate the PID1 pulses. The final gated PID spectrum was then used to select the outgoing particles of interest. One of the advantages of this setup is that data on several outgoing channels (typically ten) could be collected simultaneously. This technique was also used by Scott *et al.*[7]

The experimental energy resolution was in the range of 600–900 keV and was mainly due to kinematic broadening. The uncertainties in energy calibration were about 100 keV at low excitation energies. Despite the uncertainties in the incident beam energies and significant pulse height defects for different particles in the detectors, this accuracy was attained in the excitation energies because the calibrations were always made in the relative energy scales between peaks of known transitions. The estimated errors in absolute cross sections were about 20% due to the uncertainties in target thickness measurements, charge collection in the Faraday cup, etc.

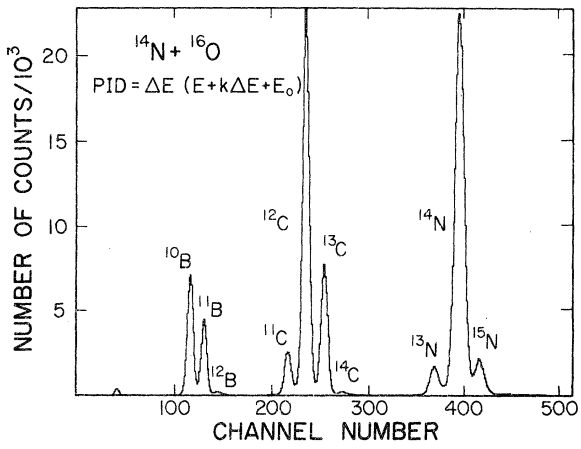

FIG. 1. Typical particle identification spectrum. The legends in the figure are self-explanatory. Note: this is a single PID spectrum.

III. EXPERIMENTAL RESULTS

A. Spectra from ^{14}N induced reactions

Figure 2 shows typical spectra for the $(^{14}N, ^{13}N)$ and $(^{14}N, ^{13}C)$ reactions on ^{12}C. The insets represent some of the low-lying levels of interest in the appropriate residual nuclei and are not necessarily drawn to scale. In principle, many of the peaks at higher excitation energies shown in the $(^{14}N, ^{13}C)$ spectra can correspond to a number of combinations of excited states in the ejectile and residual nuclei. Of course this ambiguity is removed in the $(^{14}N, ^{13}N)$ spectra since all the excited states of ^{13}N are unbound and cannot be detected by our system. The peaks are numbered in the figures for convenience.

Denoting each channel configuration by $b + B$ where b represents the ejectile nucleus and B the residual nucleus, peak 1 corresponds to $^{13}N(\mathrm{g.s.}, \frac{1}{2}^-) + ^{13}C(\mathrm{g.s.}, \frac{1}{2}^-)$ and peak 2 to $^{13}N(\mathrm{g.s.}, \frac{1}{2}^-) + ^{13}C(3.85, \frac{5}{2}^+)$ in Fig. 2(a). Similarly, in Fig. 2(b), peak 1 is due to $^{13}C(\mathrm{g.s.}, \frac{1}{2}^-) + ^{13}N(\mathrm{g.s.}, \frac{1}{2}^-)$ and peak 2 to the possible combination of $^{13}C(\mathrm{g.s.}, \frac{1}{2}^-) + ^{13}N(3.51, \frac{3}{2}^-)$ and $^{13}C(\mathrm{g.s.}, \frac{1}{2}^-) + ^{13}N(3.56, \frac{5}{2}^+)$. How-

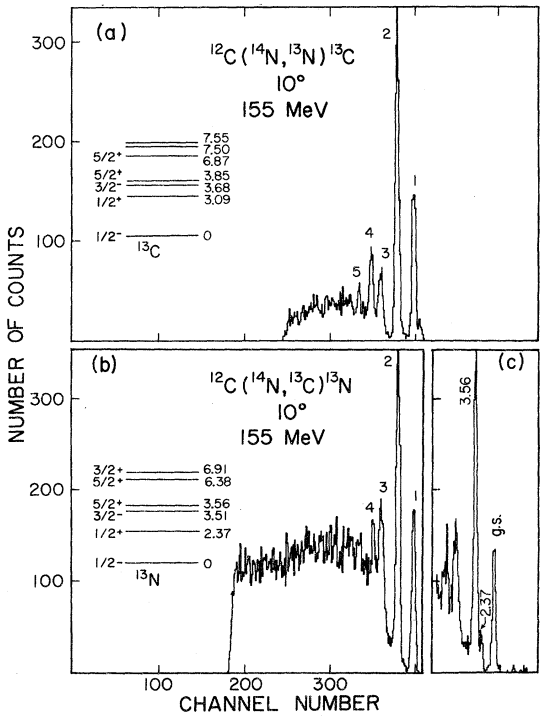

FIG. 2. Energy spectra of (a) $^{12}C(^{14}N, ^{13}N)^{13}C$ and (b) $^{12}C(^{14}N, ^{13}C)^{13}N$ reactions at $\theta_{lab} = 10°$. Insert (c) is an improved resolution spectrum, showing $^{13}N(2.37, \frac{1}{2}^+)$ state.

ever, since the $\frac{3}{2}^-$ hole state in ^{13}N is only weakly excited in a stripping reaction onto ^{12}C, peak 2 is essentially due to the 3.56 MeV ($\frac{5}{2}^+$) state in ^{13}N. The measured reduced widths[8,9] for the 3.51 MeV ($\frac{3}{2}^-$) and 3.56 MeV ($\frac{5}{2}^+$) are 0.031 and 0.21, respectively.

Other peaks which are evident from our spectra correspond to excitation energies of 7.5 MeV (peak 3), 9.5 MeV (peak 4), and 11.9 MeV (peak 5) in Fig. 2(a) and 7.2 MeV (peak 3) and 9.5 MeV (peak 4) in Fig. 2(b), respectively. However, within the errors of our energy calibration and resolution it was considered hazardous to identify these peaks with known peaks in this relatively high excitation region. Perhaps it is worthwhile to point out that they appear to be single levels rather than groups of unresolved levels since their widths are comparable to the well resolved peaks such as those corresponding to the ground state transitions. The observations of these high-lying states are certainly interesting and will be the subject of future studies.

It is evident from Figs. 2(a) and 2(b) that the first excited states in the mass-13 system [$^{13}C(3.09, \frac{1}{2}^+)$, $^{13}N(2.37, \frac{1}{2}^+)$] under consideration here are not resolved and that their intensities are low. Since considerable interest has developed recently in the spectroscopy and reaction mechanisms leading to these states,[6,10] we have tried to improve the resolution at the cost of counting rate and repeated the measurements. Even though some success was achieved in the measurements of the $^{12}C(^{14}N, ^{13}C)^{13}N(2.37, \frac{1}{2}^+)$ reaction, the analog channel reaction did not yield presentable data at this stage. An energy spectrum for the former transition from the improved measurement is shown in the insert Fig. 2(c).

In the neutron stripping reaction $^{16}O(^{14}N, ^{13}N)^{17}O$, transitions were identified to the ground state ($\frac{5}{2}^+$) and the 5.08 MeV ($\frac{3}{2}^+$) state. In addition, there were peaks observed at 7.5, 11.2, and 14.7 MeV excitation in ^{17}O. The first excited state at 0.871 MeV ($\frac{1}{2}^+$) was weakly excited and could not be clearly distinguished above the tail of the ground-state peak. In the analog channel $^{16}O(^{14}N, ^{13}C)^{17}F$ the ground state ($\frac{5}{2}^+$) and the 5.10 MeV ($\frac{3}{2}^+$) were identified together with several peaks at higher excitation energies as in the neutron stripping spectrum. There was also a peak at 3.68 MeV corresponding to the ejectile excitation in $^{13}C(\frac{3}{2}^-)$ with ^{17}F in the ground state.

The energy spectrum of the $^{16}O(^{14}N, ^{15}N)^{15}O$ reaction showed similar features to those mentioned above, but no effort was made to identify states beyond the ground-state transition because of the ambiguity associated with resolving them in this case.

B. Spectra from ^{10}B induced reactions

In the energy spectrum of the reaction $^{12}C(^{10}B, ^{11}B)^{11}C$, the ground-state transition [$^{11}B(\text{g.s.}, \frac{3}{2}^-) + ^{11}C(\text{g.s.}, \frac{3}{2}^-)$] was the strongest peak. The second peak observed at about 2 MeV excitation included two possible channels, i.e., $^{11}B(\text{g.s.}, \frac{3}{2}^-) + ^{11}C(1.99, \frac{1}{2}^-)$, and $^{11}B(2.14, \frac{1}{2}^-) + ^{11}C(\text{g.s.}, \frac{3}{2}^-)$ because of our finite energy resolution. However, the ejectile excitation, $^{11}B(2.14, \frac{1}{2}^-)$, was expected to play only a minor part since transitions from ^{10}B to the $\frac{1}{2}^-$ first excited state of ^{11}B can only proceed through transfer of a $1f$ neutron or more likely through second-order processes.[13] The spectroscopic factor for the $^{11}B(2.14) = ^{10}B + n$ state is found to be very small from (d,p) reaction studies.[11,12] Hence in the present calculations we have assumed that the process proceeds mainly through residual nuclear excitation. Several more peaks were strongly populated. However, they constitute complex transitions. For instance, a peak at about 4 MeV excitation can include $^{11}B(2.14, \frac{1}{2}^-) + ^{11}C(1.99, \frac{1}{2}^-)$, $^{11}B(\text{g.s.}, \frac{3}{2}^-) + ^{11}C(4.31, \frac{5}{2}^-)$, $^{11}B(\text{g.s.}, \frac{3}{2}^-) + ^{11}C(4.79, \frac{3}{2}^-)$, $^{11}B(4.46, \frac{5}{2}^-) + ^{11}C(\text{g.s.}, \frac{3}{2}^-)$, and $^{11}B(5.02, \frac{3}{2}^-) + ^{11}C(\text{g.s.}, \frac{3}{2}^-)$. Thus we have not attempted any analysis for these high-lying peaks. In the energy spectrum of the reaction $^{12}C(^{11}B, ^{11}C)^{11}B$, the features were almost identical, which is a natural consequence of their being analog channels.

In the reaction $^{14}N(^{10}B, ^{11}B)^{13}N$, the ground state and 3.51 MeV ($\frac{3}{2}^-$) level in ^{13}N were identified. Peaks were also observed at 7.4, 8.9, 11.9, and 14.7 MeV in the exit channel. Shell model calculations of True[14] indicate that the s-d shell admixture into the ground-state wave function of ^{14}N is only about 7%. Thus low-lying positive-parity states of ^{13}N are not expected to be excited in this reaction by a simple direct reaction mechanism. Thus the likely assignment for the 7.4 MeV state is that of the known level at 7.38 MeV ($\frac{5}{2}^-$). These assignments are consistent with the light-ion study of Hinterberger *et al.*[15] on the $^{14}N(d,t)^{13}N$ reaction. A similar situation prevails for the analog spectrum in the reaction $^{14}N(^{10}B, ^{11}C)^{13}C$. The ground state 3.68 MeV ($\frac{3}{2}^-$) and 7.55 MeV ($\frac{5}{2}^-$) states in ^{13}C were identified.

The energy spectra of the $^{14}N(^{10}B, ^{9}Be)^{15}O$ reaction showed similar features, but since the excited states of ^{9}Be are particle-unbound, the level identification here is relatively simple. The ground state ($\frac{1}{2}^-$) of ^{15}O and a peak at about 5.2 MeV, which has possible contributions from both the 5.18 MeV ($\frac{1}{2}^+$) and 5.24 MeV ($\frac{5}{2}^+$) states in ^{15}O were seen. A strong peak at 6.8 MeV was observed for which contributions from the 6.79 MeV ($\frac{3}{2}^+$) and 6.86 MeV ($\frac{5}{2}^+$) states in ^{15}O cannot be resolved.

Two additional peaks were populated at the excitation energies of 8.74 and 10.91 MeV in ^{15}O. In the reaction ^{16}O(^{10}B, ^{9}Be)^{17}F, three peaks were observed which correspond to the unresolved ground ($\frac{5}{2}^+$) and 0.5 MeV ($\frac{1}{2}^+$) first excited states in ^{17}F, and excitation energies of 5.1 and 8.1 MeV.

Finally, spectra for ^{16}O(^{10}B, ^{11}B)^{15}O and ^{16}O(^{10}B, ^{11}C)^{15}N were measured; each showed two strong peaks. They were the ground-state transitions and the transitions to the $\frac{3}{2}^-$ states in the residual nuclei, 6.18 MeV in ^{15}O and 6.32 MeV in ^{15}N. Absence of other states, which are positive-parity states, is understandable since the ^{16}O ground state is not expected to have large s-d shell components.

IV. DWBA ANALYSIS

We have assumed that all the single-nucleon transfer reactions discussed here proceed through a one-step direct process and that the distorted-wave–Born-approximation theory which fully takes into account the effects due to finite range and recoil (otherwise known as EFR DWBA) could be used to analyze the data. In order to do this, we have adopted the formulation of this theory due to Tamura.[16]

The program used for this purpose was SATURN-MARS.[1,16] This code was suitably adapted to fit an IBM 7094 computer in our laboratory with the relatively small word length (36 bits) and memory size 32 000. Test calculations and comparisons with the original version which is primarily written for the large CDC 6600 computer showed agreement to within 0.1%.

The post representation of DWBA without the inclusion of Coulomb terms in the form factor[17,18] was used throughout. A radial mesh size of 0.1 fm was found to be adequate for most of the calculations since a simple recipe is that the mesh size be less than 0.2 (π/k), where k is the asymptotic wave number in the incident and exit channels. Typically, k is in the range 4–5 fm^{-1} for the present reactions. A technique to limit the calculations of the form factor to a narrow region of $(r_b - r_a)$ space as discussed by Tamura[16] was employed. Care was taken to see that sufficient radial points have been included in the rather narrow band of values of the form factor defined around the line $r_b = (A/B)r_a$ and that in the rejected region of $(r_b - r_a)$ space the values of the form factor are negligibly small. The maximum number of partial waves included in the calculations was typically 100. For the integration of the nonlocal kernel $G_k(r_b, r_a)$ (Ref. 16) over the angle between the relative radial vectors in the incident and exit channels by Gaussian quadrature, the number of integration points was optimized. Typical values in the vicinity of 24 were used for this number. Interpolation and other techniques[1,16] were used in the program to speed up the calculations and to do them more efficiently.

A. Optical parameters

As usual in all DWBA analyses, it is important to determine the optical parameters to be used in the calculation of the distorted waves. Accordingly, elastic angular distributions were measured for all the incident channels. These are shown in Fig. 3. The statistical errors in the measurements are smaller than the size of the data points in these figures. The continuous lines are the results of six parameter optical model fits generated by a modified version of the code JIB6.[19] The corresponding values of the parameters are given in Table I. The form of the nuclear potential chosen was that of the usual Woods-Saxon type:

$$V(r) = -V\{1+\exp[(r-R_v)/a_v]\} - iW\{1+\exp[(r-R_W)/a_W]\},$$

where $R_v = r_{0v}(A_1^{1/3}+A_2^{1/3})$; $R_W = r_{0w}(A_1^{1/3}+A_2^{1/3})$. The Coulomb potential inside the nucleus was chosen to be that because of a uniformly charged sphere of radius $R_c = r_{0c}(A_1^{1/3}+A_2^{1/2})$ where the Coulomb radius parameter was chosen to be the same as that of the real radius parameter.

A well-known feature of optical model fitting to elastic data for strongly absorbed particles is the considerable ambiguities involved in such a procedure; many sets and often continuous distributions of parameters will give equally good fits.[20] Satchler[21] has illustrated the dangers of choosing best fit (i.e., minimum χ^2) results as opposed to

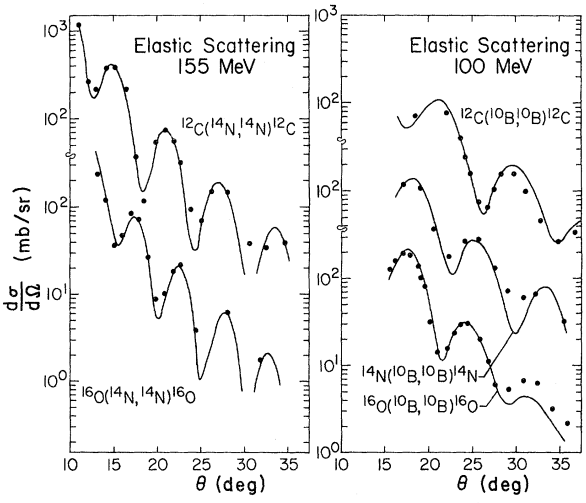

FIG. 3. Experimental elastic angular distributions and corresponding optical model fits.

TABLE I. Optical parameters.

System	E_{lab} (MeV)	V (MeV)	W (MeV)	r_{0v} (fm)	r_{0w} (fm)	a_v (fm)	a_w (fm)
$^{14}N+^{12}C$	155	100.0	38.2	0.930	1.290	0.77	0.32
$^{14}N+^{16}O$	155	100.0	39.5	0.970	1.290	0.97	0.40
$^{10}B+^{12}C$	100	81.1	66.0	1.020	1.190	0.68	0.38
$^{10}B+^{14}N$	100	28.9	14.0	1.280	1.315	0.45	0.55
$^{10}B+^{16}O$	100	14.5	6.5	1.300	1.315	0.80	0.55

reasonable fits, where by "reasonable" it is meant that the corresponding fits yield parameters which give a fair description of the inelastic and transfer processes as well. We have adopted such a point of view and have chosen only those parameters which gave reasonable descriptions in transfer channels as well at the expense of searching for the best fit in the elastic channel only. The parameters in Table I were the one used for all nucleon transfer calculations. In addition, we have made the fairly standard and simple assumption that the optical parameters to be used to describe the outgoing distorted waves are the same as the ones generated from incident channel fits. The uncertainties resulting from this assumption are unknown as usual (even though they are expected to be small) and are possible sources of error in the final results.

B. Bound state parameters

The correct choice of the bound state parameters to generate the wave functions of the transferred particle in the projectile and target is important as have been pointed out by many authors.[2,17,22] Recipes have been suggested to reduce this dependence essentially to one parameter, that is, the mean square radius $\langle r^2 \rangle$ of nuclei. However, ambiguities in the determination of $\langle r^2 \rangle$ values, and possible variations[23] of the potential from orbit to orbit, make determination of the proper choice of bound state parameters for a given situation a tedious and often ambiguous task. Thus we have adopted a fairly conventional set of bound state parameters without digging deeper into the fine points.

In our calculations, for both neutron and proton potentials, we have used the popular set $r_0 = 1.25$ fm and $a_0 = 0.65$ fm to describe the Woods-Saxon well geometry with the spin orbit potential taken to be $V_{so} = 6$ MeV and with the same geometry. These quantities were kept constant throughout. This choice was consistent with the sizes of $1p$ shell nuclei.[2,24] The depth of the binding potential was then fixed in the usual manner by requiring that the nucleon with the appropriate quantum number be bound with the known experimental separation energy.

C. Unbound states

In some instances we have done calculations on certain unbound residual nuclear states by assuming a small (0.5 MeV) binding for these states. The validity for such a weak bound state assumption in light-ion-induced reaction studies has been shown by Coker.[25] In spite of questions[26] about the validity of the same approximation in heavy-ion reactions, we proceeded to use the same recipe for the sake of simplicity with the understanding that in such cases the extracted spectroscopic factors may have larger uncertainties.

V. ANGULAR DISTRIBUTIONS

Figures 4–10 depict the experimental angular distributions and EFR DWBA calculations. All the

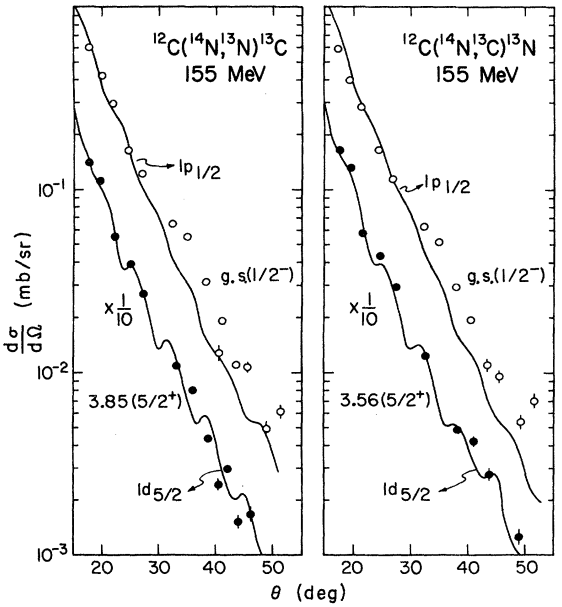

FIG. 4. Experimental and theoretical angular distributions for transfer to states of ^{13}C and ^{13}N. Solid curves are the EFR DWBA fits.

experimental angular distributions exhibit the characteristic behavior of heavy-ion reactions at very high energies i.e., extreme forward peaking and near exponential falloff. This can be understood in simple terms. For example, the grazing angle assuming undistorted Coulomb orbits (which is not valid for our case) for the specific case of 155 MeV ^{14}N ions on ^{12}C is about 7° corresponding to a grazing angular momentum of $34\hbar$. Since nuclear distortion is certainly important for our case, the effect of it will be to reduce the grazing angle even more. The larger partial waves are Coulomb scattered and we hardly see their effects while the smaller partial waves are increasingly absorbed by the nucleus. Thus the near exponential falloff of the present angular distributions is nothing but the manifestation of the absorptive part of the nuclear optical potential.

Figures 4–6 show the single-nucleon transfer angular distributions induced by 155 MeV ^{14}N beams. The transition to the ground states of ^{13}C (Fig. 4), ^{13}N (Fig. 4), and ^{15}O (Fig. 5) are well reproduced by theoretical calculations with transfer between $1p_{1/2}$ shells. Similarly, the experimental angular distribution for the $\frac{5}{2}^+$ states in both ^{13}N and ^{13}C are very well reproduced by theory. For the ^{16}O target, the proton and neutron transfers to the ground and first excited states of both ^{17}O and ^{17}F are shown in Fig. 5. The contribution of the $2s_{1/2}$ first excited state to the calculated cross section was small even after assuming full single particle strength for this orbital and did not in-

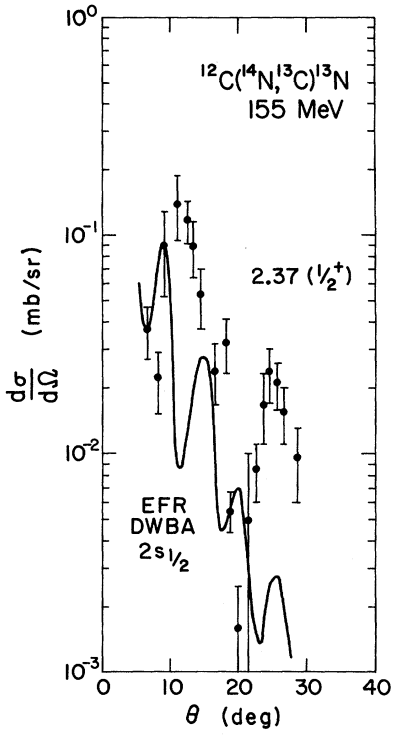

FIG. 6. Experimental and theoretical angular distributions for transfer to the ^{13}N(2.37, $\frac{1}{2}^+$) state through the ^{12}C(^{14}N, ^{13}C)^{13}N reaction.

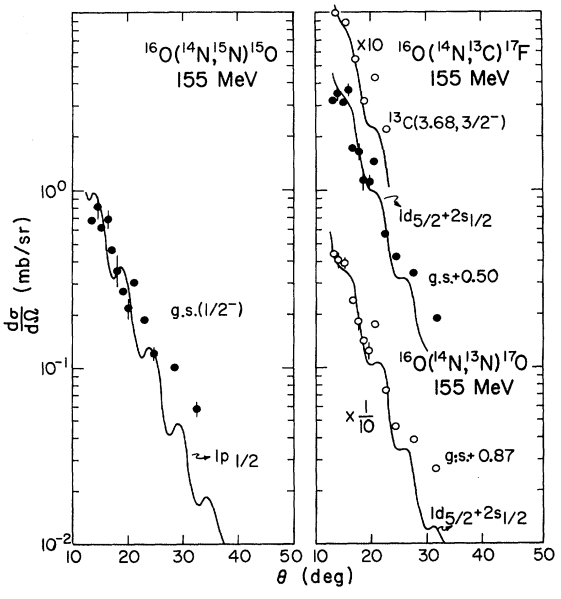

FIG. 5. Experimental and theoretical angular distributions for transfers to states of ^{15}O, ^{17}F, and ^{17}O. The ejectile excitation ^{13}C(3.68, $\frac{3}{2}^-$) is also shown.

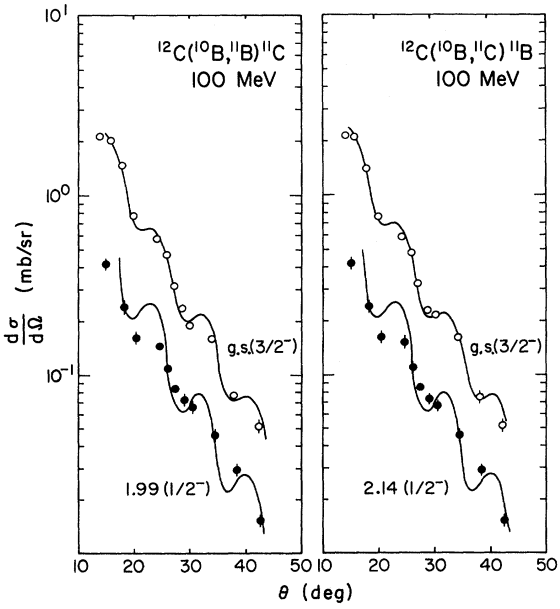

FIG. 7. Experimental and theoretical angular distributions for transfers to states of ^{11}C and ^{11}B.

fluence the extracted value for the ground-state $1d_{5/2}$ spectroscopic factor appreciably. In Fig. 5 is also shown the experimental angular distribution and corresponding theoretical calculation for ejectile excitation $^{13}C(3.68, \frac{3}{2}^-)$ leaving the ^{17}F nucleus in its ground state. All the fits shown in Figs. 4 and 5 are quite good. The only conspicuous exception in this series of reactions seems to be the transfer to the first excited state in ^{13}N, i.e., the $^{12}C(^{14}N, ^{13}C)^{13}N(2.37, \frac{1}{2}^+)$ reaction. Anomalous angular distributions quite similar to Fig. 6 have been reported elsewhere.[6,10,27] As has been agreed in these references, the calculated angular distribution is completely out of phase with the experimental result. The solution to this puzzle is still not known and more theoretical effort would be useful. The nearly identical spectroscopic factors extracted for the $^{13}C(3.85, \frac{5}{2}^+)$ which is bound and the analog state $^{13}N(3.56, \frac{5}{2}^+)$ which is unbound, but for which we made the weak bound state assumption coupled with the excellent fits shown in Fig. 4 for these states, bolster our confidence in the reliability of the simple procedure we have adopted for some of these unbound cases.

The experimental angular distributions and corresponding EFR DWBA calculations for the ^{10}B-induced reactions are shown in Figs. 7–10. Due to the particular geometry chosen for the reactions on the ^{12}C target in making comparisons with data, the theoretical angular distributions had to be corrected to include angular acceptances according to particular experimental setups. The fits to the ground-state transfers to ^{11}C and ^{11}B (Fig. 7) are excellent assuming transfer between $1p_{3/2}$ nucleons. As discussed in Sec. III, the first excited state angular distributions are expected to be predominantly those due to $^{12}C(^{10}B, ^{11}B[g.s.])$-$^{11}C(1.99, \frac{1}{2}^-)$ (Fig. 7) and $^{12}C(^{10}B, ^{11}C[g.s.])$-

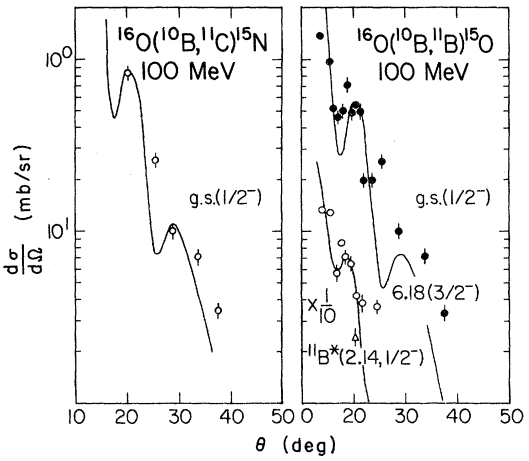

FIG. 9. Experimental and theoretical angular distribution for transfers to states of ^{15}N and ^{15}O. Ejectile excitation corresponding to the $^{11}B^*(2.14, \frac{1}{2}^-)$ state and $^{15}O(g.s., \frac{1}{2}^-)$ residual state is indicated by the triangle.

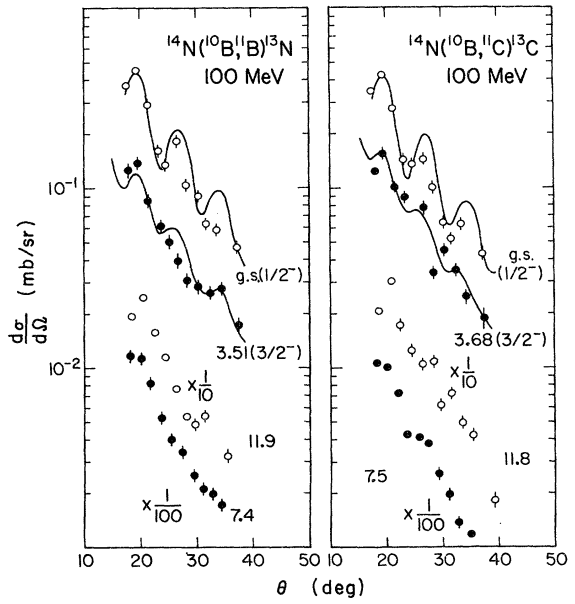

FIG. 8. Experimental and theoretical angular distributions for transfers to states of ^{13}N and ^{13}C. The experimental angular distributions for the peaks around 7.4 and 11.9 MeV excitation are also shown.

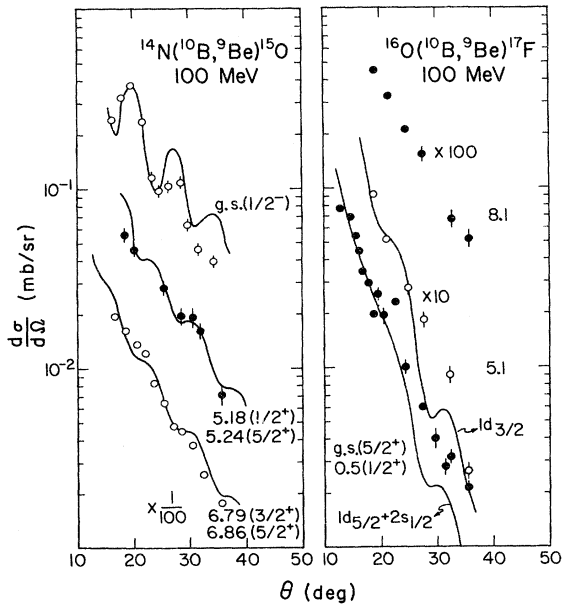

FIG. 10. Experimental and theoretical angular distributions for transfers to states of ^{15}O and ^{17}F via one-proton stripping reactions. The experimental angular distribution for the peak at 8.1 MeV excitation in ^{17}F is also shown.

^{11}B(2.14, $\frac{1}{2}^-$) (Fig. 7), respectively. The angular distributions for these states again show reasonable correspondence with theoretical predictions.

Figure 8 depicts the angular distribution resulting from the (^{10}B, ^{11}B), (^{10}B, ^{11}C) analog reactions on ^{14}N. Theoretical calculations for the pickup of a $1p_{1/2}$ nucleon from ^{14}N leading to ^{13}N(g.s.) and ^{13}C as well as for the pickup of a $1p_{3/2}$ nucleon leading to ^{13}N(3.51) and ^{13}C(3.68) are indicated by continuous lines in Fig. 8. Due to the ambiguities in the exit channel level identifications at higher energies, we have not done calculations on these states.

Figure 9 shows the angular distributions to the residual nuclear states through the (^{10}B, ^{11}C), (^{10}B, ^{11}B) analog reactions on ^{16}O. The differential cross section at 20° obtained in a good resolution study for the ejectile excitation corresponding to the reaction ^{16}O(^{10}B, ^{11}B*[2.14, $\frac{1}{2}^-$])^{15}O(g.s.) is also shown in Fig. 9 (triangle with error bar).

Angular distributions to states in ^{15}O and ^{17}F via the proton stripping reaction (^{10}B, ^{9}Be) are shown in Fig. 10. The fit to the ground state of ^{15}O is good. For the unresolved states at 5.18($\frac{1}{2}^+$) and 5.24($\frac{5}{2}^+$), the contribution from the $\frac{1}{2}^+$ state was found to be quite small (about 5%) even assuming full strength for this state. Thus the spectroscopic factor extracted is relatively reliable and can be considered entirely due to the 5.24($\frac{5}{2}^+$) state within errors. For the theoretical calculation shown for the unresolved states at 6.79 MeV ($\frac{3}{2}^+$) and 6.86 MeV ($\frac{5}{2}^+$), the spectroscopic factors were assumed to be those given by Halbert and French[28] (i.e., 0.47 for the $\frac{3}{2}^+$ state and 0.63 for the $\frac{5}{2}^+$ state) with an over-all normalization of 0.8.

In the calculations for ^{17}F states, the contribution to the calculation from the first excited state at 0.5 MeV ($\frac{1}{2}^+$) was again found to be very small even assuming maximum strength for this state. The general shape of the 5.1 MeV ($\frac{3}{2}^+$) angular distribution fits the data reasonably well with the unbound state recipe mentioned before.

VI. SPECTROSCOPIC FACTORS

Tables II and III summarize the product spectroscopic factors $C_1^2S_1C_2^2S_2$ extracted from the present analyses and other relevant information for the transitions observed in the $1p$ and $2s$-$1d$ shells, respectively. Similarly Figs. 11 and 12 represent the C^2S values for the residual nuclei obtained for the $1p$ and $2s$-$1d$ shells. It should be emphasized that in extracting these values for the residual nuclei, the spectroscopic factors for the projectile-ejectile system (always in the $1p$ shell) were assumed to be the same as those predicted by Cohen and Kurath.[29]

As is evident from Fig. 11 and Table II, the spectroscopic factors extracted for the $1p$ shell from the present study are in good agreement

TABLE II. Spectroscopic factors in the $1p$-shell.

Reaction	E_x (MeV)	Single-particle orbitals (a,b)	Single-particle orbitals (A,B)	l transfer	$C_1^2S_1C_2^2S_2$ Present	$C_2^2S_2$ [a] Present	$C_2^2S_2$ Other
^{12}C(^{14}N, ^{13}N)^{13}C	0.00	$1p_{1/2}$	$1p_{1/2}$	0, 1	0.50	0.72	0.61 [b], 0.8 [c] 0.58 [d], 0.81 [e]
^{12}C(^{14}N, ^{13}C)^{13}N	0.00	$1p_{1/2}$	$1p_{1/2}$	0, 1	0.43	0.62	0.61 [b], 0.53 [d]
^{16}O(^{14}N, ^{15}N)^{15}O	0.00	$1p_{1/2}$	$1p_{1/2}$	0, 1	2.90	2.00	1.8–3.2 [f], 2.2 [g]
^{14}N(^{10}B, ^{11}B)^{13}N	0.00	$1p_{3/2}$	$1p_{1/2}$	1, 2	0.79	0.72	0.69 [b]
	3.51 [h]	$1p_{3/2}$	$1p_{3/2}$	0, 1, 2	0.21	0.19	0.14 [b]
^{14}N(^{10}B, ^{11}C)^{13}C	0.00	$1p_{3/2}$	$1p_{1/2}$	1, 2	0.68	0.62	0.8, 0.88 [f], 0.69 [b]
	3.68	$1p_{3/2}$	$1p_{3/2}$	0, 1, 2	0.24	0.22	0.14 [b]
^{14}N(^{10}B, ^{9}Be)^{15}O	0.00	$1p_{3/2}$	$1p_{1/2}$	1, 2	0.65	1.08	1.43 [b]
^{12}C(^{10}B, ^{11}B)^{11}C	0.00	$1p_{3/2}$	$1p_{3/2}$	0, 1, 2	2.85	2.61	2.85 [b], 2.86 [i]
	1.99	$1p_{3/2}$	$1p_{1/2}$	1, 2	0.60	0.55	0.75 [b], 0.28 [i]
^{12}C(^{10}B, ^{11}C)^{11}B	0.00	$1p_{3/2}$	$1p_{3/2}$	0, 1, 2	2.58	2.36	2.6 [j], 2.98 [k], 2.85 [b]
	2.14	$1p_{3/2}$	$1p_{1/2}$	1, 2	0.48	0.44	0.75 [b], 0.78 [k]
^{16}O(^{10}B, ^{11}B)^{15}O	0.00	$1p_{3/2}$	$1p_{1/2}$	1, 2	1.27	1.17	1.8–3.2 [f], 2.2 [g]
^{16}O(^{10}B, ^{11}C)^{15}N	0.00	$1p_{3/2}$	$1p_{1/2}$	1, 2	1.65	1.51	2.14 [l]

[a] Assuming $C_1^2S_1$ given by Cohen and Kurath (Ref. 29).
[b] See Ref. 29.
[c] See Ref. 31.
[d] See Ref. 33.
[e] See Ref. 34.
[f] See Ref. 35.
[g] See Ref. 36.
[h] Unbound.
[i] Average of values quoted by Ref. 44 for energy independent W.
[j] See Ref. 30.
[k] See Ref. 15.
[l] See Ref. 32.

TABLE III. Spectroscopic factors in the $2s$-$1d$ shell.

Reaction	E_x (MeV)	Single-particle orbitals (a,b)	Single-particle orbitals (A,B)	l transfer	$C_1^2S_1C_2^2S_2$ Present	$C_2^2S_2$ [a] Present	$C_2^2S_2$ Other
$^{12}C(^{14}N, ^{13}N)^{13}C$	3.85	$1p_{1/2}$	$1d_{5/2}$	2, 3	0.39	0.57	0.8 [b], 0.37 [c]
$^{12}C(^{14}N, ^{13}C)^{13}N$	2.37 [d]	$1p_{1/2}$	$2s_{1/2}$	1	0.06	0.09	
	3.56 [d]	$1p_{1/2}$	$1d_{5/2}$	2, 3	0.34	0.49	
$^{16}O(^{14}N, ^{13}N)^{17}O$	0.00	$1p_{1/2}$	$1d_{5/2}$	2, 3	0.48 [e]	0.69	0.81 [f], 0.8–1.0 [g]
$^{16}O(^{14}N, ^{13}C)^{17}F$	0.00	$1p_{1/2}$	$1d_{5/2}$	2, 3	0.41 [e]	0.59	0.9 [h]
$^{16}O(^{14}N, ^{13}C^*)^{17}F$	3.68	$1p_{3/2}$	$1d_{5/2}$	1, 2, 3	0.15	0.59 [i]	
$^{14}N(^{10}B, ^{9}Be)^{15}O$	5.24	$1p_{3/2}$	$1d_{5/2}$	1, 2, 3	0.025 [e]	0.04	0.06 [j], 0.04–0.06 [k] 0.05 [l]
$^{16}O(^{10}B, ^{9}Be)^{17}F$	0.00	$1p_{3/2}$	$1d_{5/2}$	1, 2, 3	0.25 [e]	0.42	0.9 [h], 0.85–1.05 [m]
	5.10 [d]	$1p_{3/2}$	$1d_{3/2}$	1, 2, 3	0.13	0.22	

[a] Assuming $C_1^2S_1$ given by Cohen and Kurath (Ref. 29).
[b] See Ref. 31.
[c] See Ref. 6.
[d] Unbound.
[e] Contribution from nearby $s_{1/2}$ state approximately 5% from theoretical calculations.
[f] See Ref. 39.
[g] See Ref. 40.
[h] See Ref. 41.
[i] This value gives $C_1^2S_1 = 0.23$ for $^{14}N = {}^{13}C(3.68) + p$.
[j] See Ref. 28.
[k] See Ref. 37.
[l] See Ref. 38.
[m] See Ref. 42.

with the intermediate coupling calculations of Cohen and Kurath.[29] The results of DeVries[30] from heavy-ion reaction studies and those of other authors[31-36] from light-ion reaction studies are also given in Table II and Fig. 11 for comparison. Due to the vast amount of data and analysis available in literature on spectroscopic studies with light ions on light nuclei in the region in which we are interested, an exhaustive comparison, of course, is impossible. Hence we have picked out essentially samplings of other works for comparison.

Perhaps it is well worth commenting at this point that a comparison of the spectroscopic factors obtained from the present study and of those from light-ion reactions could be clouded by differences in bound state parameters used and the wide variety

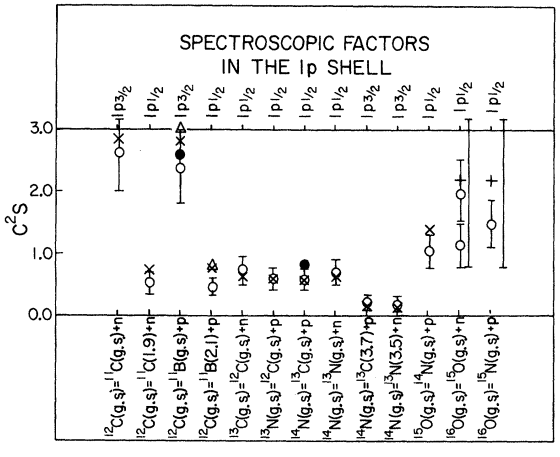

FIG. 11. Spectroscopic factors extracted for the $1p$ shell. Open circles are the present results. The error bars indicate the uncertainties in the extraction of S and is an approximate estimate based on experimental and theoretical uncertainties. The ×'s are the theoretical predictions of Cohen and Kurath (Ref. 29). The other symbols have the following meaning: , Ref. 30; △, Ref. 15; +, Ref. 36. The vertical lines in the last columns represent the range of values from Ref. 35.

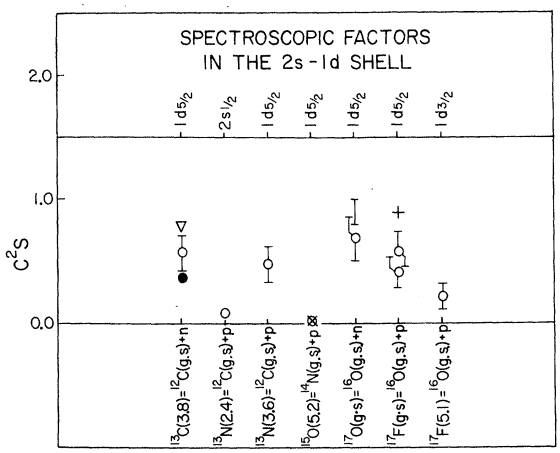

FIG. 12. Spectroscopic factors extracted for the $2s$-$1d$ shell. Open circles and error bars represent the present results with our estimated uncertainties. The other symbols have the following meaning: ▽, Ref. 6; , Ref. 31; +, Ref. 41. The vertical line represents range of results reported in Ref. 40.

of procedures which enter into some of the light-ion analyses (e.g., arbitrary normalizations, lower radial cutoff approximations, inclusion or noninclusion of finite range and nonlocal effects, etc.). Nevertheless, we quote these results also with the hope that an over-all agreement to within about 30% may be considered significant.

Figure 12 and Table III summarize the spectroscopic information obtained for states in the $2s$-$1d$ shells. Again, the results extracted from the present data and from those of other authors[6,31,37-42] are presented for comparison. It is interesting to note that the present results indicate that there is a consistent depletion of the single-particle strengths of the ground states of ^{17}O and ^{17}F as reflected by the spectroscopic factors in the vicinity of 0.6, whereas the light-ion results are generally about 0.8–1.0. Brown, Evans, and Thouless[43] predict that a depletion of the simple single-particle levels in the region by as much as 25% is possible because of the coupling of the particle with odd-parity vibrations. The very small spectroscopic factors for the $2s_{1/2}$ first excited state in ^{13}N (even in spite of the rather arbitrary normalization) and its possible consequences have been discussed elsewhere.[27]

VII. SUMMARY AND CONCLUSIONS

We have collected and analyzed heavy-ion transfer data at high energies populating levels mainly in the $1p$ and $2s$-$1d$ shells. It appears that heavy-ion-induced one-nucleon transfer reactions from the present analysis could be legitimately used to extract meaningful spectroscopic information in the light-mass region and at very high incident energies. The associated uncertainties which are in most cases characteristic of the DWBA formalism are not significantly different from those associated with light-ion studies. However, the dynamics of the reactions must be treated correctly, e.g., via the use of full finite range DWBA codes including recoil effects. However, occasional anomalies do arise such as that connected with the transfer to the ^{13}N$(2.37, \frac{1}{2}^+)$ case. In such instances, possibilities such as excitations in the incident and/or exit channels should also be included in the calculations before meaningful structure information can be obtained. In view of the persistent anomalies reported in the literature for the first $\frac{1}{2}^+$ states in the mass-13 nuclei ^{13}N and ^{13}C, it would be very worthwhile to pursue the study of the first $\frac{1}{2}^+$ states systematically in this mass region. It is certainly feasible and also desirable to extend the formulation to include multinucleon cluster transfer in this mass and energy region and exploit the selectivity and ability to excite high angular momentum states in relatively high excitation regions which might give interesting insights into unusual nuclear configurations. Such projects are of course widely undertaken by many groups of investigators including us. In addition, less well studied processes such as successive transfers[45] and mutual excitations might also start playing important roles in future multinucleon transfer studies.

ACKNOWLEDGMENTS

We would like to express our appreciation to Taro Tamura for many valuable discussions. One of the authors (KGN) would like to thank Low Kum Sang for his generous help in connection with the adaptation of the computer code SATURN-MARS and Dieter Kurath for a private communication. The discussions with A. Bacher during the course of these experiments have been of considerable value to us. Finally, we thank Fritz Siller, Roy Hanus, and V. Ray Koym for their help in connection with the experimental setups.

---

*Work supported in part by the National Science Foundation.

†Permanent address: Physikalisches Institut der Universität-Erlangen Nürnberg, Erlangen, Germany; Max Kade Foundation Fellow.

[1]T. Tamura and K. S. Low, Phys. Rev. Lett. 31, 1356 (1973); K. S. Low and T. Tamura, Phys. Lett. B 48B, 285 (1974).

[2]J. L. C. Ford, K. S. Toth, G. R. Satchler, D. C. Hensley, L. W. Owen, R. M. DeVries, R. M. Gaedke, P. J. Riley, and S. T. Thornton, Phys. Rev. C 10, 1429 (1974).

[3]F. D. Becchetti, B. G. Harvey, D. Kovar, J. Mahoney, and M. S. Zisman, Phys. Rev. C 10, 1846 (1974), and references therein.

[4]N. Anyas-Weiss, J. C. Cornell, P. S. Fisher, P. N. Hudson, A. Menchaca-Rocha, D. J. Millener, A. D. Panagiotou, D. K. Scott, D. Strottman, D. M. Brink, B. Buck, P. J. Ellis, and T. Engeland, Phys. Rep. 12C, 201 (1974).

[5]W. von Oertzen, M. Liu, C. Caverzasio, J. C. Jacmart, F. Pougheon, M. Riou, J. C. Roynette, and C. Stephen, Nucl. Phys. A A143, 34 (1970).

[6]R. M. DeVries, M. S. Zisman, J. G. Cramer, K. L. Liu, F. D. Becchetti, B. G. Harvey, H. Homeyer, D. G. Kovar, J. Mahoney, and W. von Oertzen, Phys. Rev. Lett. 32, 680 (1974).

[7]D. K. Scott, P. N. Hudson, P. S. Fisher, C. U. Cardinal, N. Anyas-Weiss, A. D. Panagiotou, P. J. Ellis, and B. Buck, Phys. Rev. Lett. 28, 1659 (1972).

[8]T. Lauritsen and F. Ajzenberg-Selove, *Energy Levels of Light Nuclei* (National Academy of Sciences - Research Council, Washington, D. C., 1962).
[9]H. T. Fortune, T. J. Gray, W. Trost, and N. R. Fletcher, Phys. Rev. 179, 1033 (1969).
[10]K. G. Nair, H. Voit, M. Hamm, C. Towsley, and K. Nagatani, Phys. Rev. Lett. 33, 1588 (1974).
[11]D. M. Bilaniuk and J. C. Hensel, Phys. Rev. 120, 211 (1960).
[12]S. Hinds and R. Middleton, Nucl. Phys. 38, 114 (1962).
[13]D. Kurath (private communication).
[14]W. W. True, Phys. Rev. 130, 1530 (1963).
[15]F. Hinterberger, G. Mairle, U. Schmidt-Rohr, P. Turek, and G. J. Wagner, Nucl. Phys. A A106, 161 (1968).
[16]T. Tamura, Phys. Rep. 14C, 59 (1974).
[17]K. G. Nair, J. S. Blair, W. Reisdorf, W. R. Wharton, W. J. Braithwaite, and M. K. Mehta, Phys. Rev. C 8, 1129 (1973).
[18]R. M. DeVries, G. R. Satchler, and J. G. Cramer, Phys. Rev. Lett. 32, 1377 (1974).
[19]G. Lerner, Texas A&M University, JIB-6 (unpublished).
[20]J. S. Blair, in *Proceedings of the International Conference on Reactions Induced by Heavy Ions, Heidelberg, Germany,* edited by R. Bock and W. Hering (North-Holland, Amsterdam, 1970).
[21]G. R. Satchler, in *Proceedings of the International Conference on Reactions between Complex Nuclei, Nashville, Tennessee,* edited by R. L. Robinson, F. K. McGowan, J. B. Ball, and J. H. Hamilton (North-Holland, Amsterdam/American Elsevier, New York, 1974).
[22]J. P. Schiffer and H. J. Körner, Phys. Rev. C 8, 841 (1973); Phys. Rev. Lett. 27, 1457 (1971).
[23]J. W. Negele, Phys. Rev. C 1, 1260 (1970); 9, 1054 (1974).
[24]D. H. Wilkinson and M. E. Mafethe, Nucl. Phys. 85, 97 (1966).
[25]W. R. Coker, Phys. Rev. C 9, 784 (1974).
[26]L. Ray, W. R. Coker, and T. Udagawa (unpublished). However, even for heavy-ion reactions, the validity of this assumption depends on the state considered. For example, relatively large differences exist between the weak bound state assumption and the Gamow state calculation for the ^{13}N(2.37, $\frac{1}{2}^+$) state, whereas the difference is much smaller and relatively more acceptable for spectroscopic purposes for the ^{13}N(3.56, $\frac{5}{2}^+$); L. Ray (private communication), L. Ray *et al.*, Bull. Am. Phys. Soc. 20, 717 (1975).
[27]K. G. Nair, M. Hamm, C. W. Towsley, R. Hanus, and K. Nagatani, in Second International Conference on Clustering Phenomena in Nuclei, University of Maryland, April 1975 (unpublished).
[28]E. C. Halbert and J. B. French, Phys. Rev. 105, 1563 (1957).
[29]S. Cohen and D. Kurath, Nucl. Phys. A A101, 1 (1967).
[30]R. M. DeVries, Phys. Rev. C 8, 951 (1973).
[31]R. N. Glover and A. D. W. Jones, Nucl. Phys. 84, 673 (1966).
[32]J. C. Hiebert, E. Newman, and R. H. Bassel, Phys. Rev. 154, 898 (1967).
[33]C. A. Pearson, J. M. Covan, D. Zissermann, T. G. Miller, F. P. Gibson, R. Haglund, W. Morrison, and G. Westley, Nucl. Phys. A A191, 1 (1972).
[34]J. P. Schiffer, G. C. Morrison, R. H. Siemssen, and B. Zeidman, Phys. Rev. 164, 1274 (1967).
[35]J. L. Snelgrove and E. Kashy, Phys. Rev. 187, 1246 (1969).
[36]D. Bachelier, M. Bernas, I. Brissaud, C. Detraz, and P. Radvanyi, Nucl. Phys. A A126, 60 (1969).
[37]W. Bohne, H. Homeyer, H. Morgenstern, and J. Scheer, Nucl. Phys. A A113, 97 (1968).
[38]W. P. Alford and K. H. Purser, Nucl. Phys. A A132, 86 (1969).
[39]F. Ajzenberg-Selove, Nucl. Phys. A A166, 81 (1971).
[40]M. D. Cooper, W. F. Hornyak, and P. G. Roos, Nucl. Phys. A A218, 249 (1974).
[41]S. T. Thornton, Nucl. Phys. A A137, 531 (1969).
[42]C. J. Oliver, P. D. Forsyth, J. L. Hutton, G. Kaye, and J. R. Mines, Nucl. Phys. A A127, 567 (1969).
[43]G. E. Brown, J. A. Evans, and D. J. Thouless, Nucl. Phys. 45, 164 (1963).
[44]T. G. Gray, H. T. Fortune, W. Trost, and N. R. Fletcher, Nucl. Phys. A A144, 129 (1970).
[45]D. Robson, Comments Nucl. Part. Phys. 6, 1 (1974).